Sensors and Actuators A xxx (2011) xxx–xxx

Contents lists available at ScienceDirect

Sensors and Actuators A: Physical

journal homepage: www.elsevier.com/locate/sna

A probe with ultrathin film deflection sensor for scanning probe microscopy and material characterization

Angelo Gaitas [a,b,*], Tao Li [a], Weibin Zhu [a]

[a] PicoCal, Inc., 333 Parkland Plaza, Ann Arbor, MI 48103, United States
[b] Delft University of Technology, Mekelweg 4, 2628CD Delft, The Netherlands

A R T I C L E I N F O

Article history:
Received 7 January 2011
Received in revised form 4 April 2011
Accepted 12 April 2011
Available online xxx

Keywords:
Scanning probe microscope
Piezoresistive sensor
Microcantilever
Elastography
Material characterization
Mechanical characterization

A B S T R A C T

We report a microcantilever probe with a 5 nm gold deflection sensor for the study of local mechanical properties such as adhesion and elasticity on a sample. The probe has a dynamic range of tens of microns, which allows for a deeper insight into the mechanical properties of materials. The gauge factor of the piezoresistive sensor is 4.1 ± 0.1 and the deflection sensitivity is 0.1 ppm/nm. Noise analysis indicates a minimum detectable deflection of ≈0.7 nm. Topographical scans are demonstrated. Studies of adhesion and stiffness of two different samples demonstrate the usefulness of the probe in the investigation of local mechanical properties.

© 2011 Elsevier B.V. All rights reserved.

1. Introduction

Microcantilevers are used in a number of applications including atomic-force microscopy (AFM) [1], nanolithography [2], high-density data storage [3,4], biological sensing [5], cell elastography [6], measurement of material properties such as adhesion, stiffness, elasticity and viscosity [7], and explosives detection [8]. Piezoresistive deflection-sensing elements are integrated onto micromachined cantilevers to increase sensitivity, and reduce complexity and cost. These sensing elements are made by selectively doping silicon [9–11], by depositing and patterning metal or metal oxide films, such as gold [12–14], indium tin oxide [15,16], and nichrome [17], or by depositing and patterning other materials such as amorphous carbon [18].

Compared with doped-silicon sensing elements, deposited metal film elements have important advantages including simplified fabrication, a lower manufacturing cost [19], and the capability to scale down to smaller dimensions while maintaining sensitivities [12]. Metallic sensing elements also enable the use of alternative substrate materials (such as polymers), that tend to exhibit higher compliance properties and improved thermal isolation [19,20]. Metal film sensing elements with thickness larger than 10 nm typically have gauge factors of about 2 or smaller [12,13,20,22]. Ultrathin metal film sensing elements with thickness less than 10 nm have demonstrated increased piezoresistive sensitivity [21].

In this work, probes with metal ultrathin film sensors on silicon substrates for scanning probe microscopy and material characterization are developed. The probes operate without the need of a complicated optical lever required by AFM systems. In addition, the probes have a very large dynamic range of tens of microns. This feature enables monitoring movement of tens of microns in the out-of-plane axis (*Z*-axis), which allows for a deeper insight into the mechanical properties of materials. For example, the adhesive forces on a surface can be studied in greater detail in order to characterize materials by monitoring the full range of the rupture force which is required to break the adhesion from the surface. These probes are also suitable for biological scanning in liquid environments by adding a thin insulating layer over the exposed metal film, overcoming the limitations of the optical lever on AFM caused by the laser refraction at the non-static liquid–air interface during scanning in liquids. Finally, compared with other approaches such as optical lever detection and piezoelectric pick-up, piezoresistive sensing is relatively simple to expand to a one or two dimensional probe array for higher throughput multi-location measurements.

2. Theory

The change in resistance, ΔR, can be converted into the corresponding force exerted on the piezoelectric sensor using the gauge

* Corresponding author at: PicoCal, Inc., 333 Parkland Plaza, Ann Arbor, MI 48103, United States. Tel.: +1 734 913 2608; fax: +1 734 619 6676.
E-mail address: angelo@picocal.com (A. Gaitas).

0924-4247/$ – see front matter © 2011 Elsevier B.V. All rights reserved.
doi:10.1016/j.sna.2011.04.023

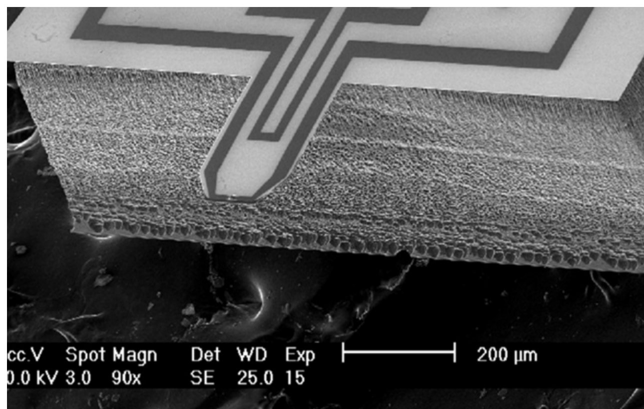

Fig. 1. SEM image of a piezoresistive probe developed in this effort. The shorter element near the base is the piezoresistive element. The longer metal element that goes over the tip is a thermal element used for heating and measuring temperature related parameters (not used in the work reported here).

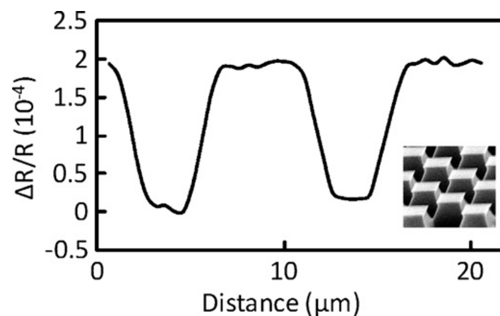

Fig. 2. Measured $\Delta R/R$ vs. in-plane scanning displacement in a 20 μm line scan over a 10 μm-pitch square grating with 1 μm height (shown in the inset).

factor. The gauge factor of the metal piezoresistive sensor is given by the following equation

$$\frac{\Delta R}{R} = \frac{K}{E}\sigma \tag{1}$$

where K is the gauge factor, E is Young's modulus of the cantilever material, and σ is the average stress of the metal sensor. The average stress of the sensor can be estimated using cantilever analysis [23,24]. The overall equation thus becomes

$$\frac{\Delta R}{R} = \frac{3}{2}k\frac{(L-\lambda/2)t}{L^3}\Delta z \tag{2}$$

where λ is the length of the piezoresistor, L and t are the length and thickness of the cantilever, Δz is the displacement of the cantilever at the tip. The deflection sensitivity is defined by solving Eq. (2) for $(\Delta R/R)/\Delta z$, and its value can be experimentally calculated from the slope of $(\Delta R/R)$ vs. Δz.

3. Device fabrication

Fig. 1 shows the probe developed in this effort. The design includes two sensing elements on one cantilever, each of which consists of a 5 nm gold film located on a silicon cantilever. The resistor covering the tip area forms a microbolometer and the resistor near the base of the cantilever forms the deflection sensing element. The rectangular cantilever is 200 μm wide, 300 μm long, and 2 μm thick. The pyramid shaped tip is 7.5 ± 0.5 μm high and has a tip diameter of 200 nm. The cantilever is a stacked structure of silicon and silicon oxide layers. A 3 mm × 1.4 mm × 0.5 mm chip serves as the base of the cantilever.

The device is fabricated in a four-mask process. The process starts with a silicon-on-insulator (SOI) wafer. A thermal oxide masking layer is deposited and patterned for the probe tip. The tip is formed using timed KOH anisotropic etching. The oxide mask is then removed and the tip is sharpened with several oxide sharpening steps [25]. A 100 nm-thick silicon oxide is thermally grown on the wafer to provide electrical insulation. The cantilever is patterned on the front side of the wafer with the Bosch deep reactive-ion etching (DRIE) process. Metal lines are evaporated and patterned on top of the cantilever structure with lift-off process to form the sensing elements. The thicknesses of the metal layers are monitored during the evaporation and the variation between process runs is within ±10%. The chip is then shaped by a back side DRIE process with an etch rate of 3 μm/min. The buried oxide layer of the SOI wafer acts as an etch stop to prevent the back side DRIE from attacking the Si cantilever structures. Finally, the probes are released by removing the buried oxide layer using buffered HF etchant.

4. Experimental results and discussion

The change in resistance of the sensing element with cantilever deflection is directly measured using a micro-Ohm meter (Agilent, HP-34420A), without the need of an interface amplifying circuit, and the data is acquired with a LabView program. A piezoelectric *XYZ* stage with 100 μm range and nanometer resolution on each axis (PiezoJena, Tritor 100) is used to move the sample underneath the probe.

The overall resistance of the sensing element is ≈1773 Ω. The parasitic resistance of the inactive portions of the metal-line resistor can be calculated using the geometry and the measured sheet resistance. Additional resistances from the cabling and the wirebonding are less than 1 Ω and therefore do not have a significant contribution to the overall resistance. Thus, the active piezoresistive sensing part of the sensing element has a resistance of ≈516 Ω.

The noise performance of the sensor is evaluated by biasing the metal-film resistor with the built-in battery-based power source in a low-noise current preamplifier (Stanford Research Systems SR570). The output voltage of the current preamplifier is then fed into a spectrum analyzer (Agilent 4395A) for noise measurement. No 1/f noise was observed between the frequency range from 10 Hz (equipment limitation) to 1 kHz, and the white noise floor was found to be $\approx 22\,\mathrm{nV}/\sqrt{\mathrm{Hz}}$. This is ≈3 times higher than the calculated Johnson noise spectrum based on the nominal overall resistance of the sensing element, and may be related to the thermal vibration noise of the cantilever. The minimum detectable deflection is given by

$$\Delta z_{\min} = \frac{\overline{V_n}/I_{Bias}}{R}\cdot\frac{1}{s_z} \tag{3}$$

where $\overline{V_n}$ is the total noise voltage over the measurement bandwidth (≈30 Hz from the micro-ohm meter), I_{Bias} is the bias current used in the resistance measurement (1 mA or less), R is the nominal resistance of the sensing element, and s_z is the sensitivity of the piezoresistive sensor defined as $\Delta R/R/\Delta z$ and obtained by experiments as discussed below. The total noise of the micro-ohm meter is a lot less that the noise from the device and it is been ignored in the calculation. Thus the minimum detectable deflection is ≈0.7 nm.

Fig. 2 shows a 20 μm line scan over the top surface of a 10 μm pitch square grating with 1 μm height. The curve in Fig. 2 is the plot of the change in resistance, $\Delta R/R$, vs. the in-plane (*XY* plane) movement, and shows the scanned surface profile of the grating. A 1 μm change in the deflection of the cantilever tip corresponds to an approximately 0.1 Ω change in resistance.

The attractive and repulsive forces between a probe tip and sample surface are of interest as they can provide information about mechanical properties of the probe and of the sample (such as adhe-

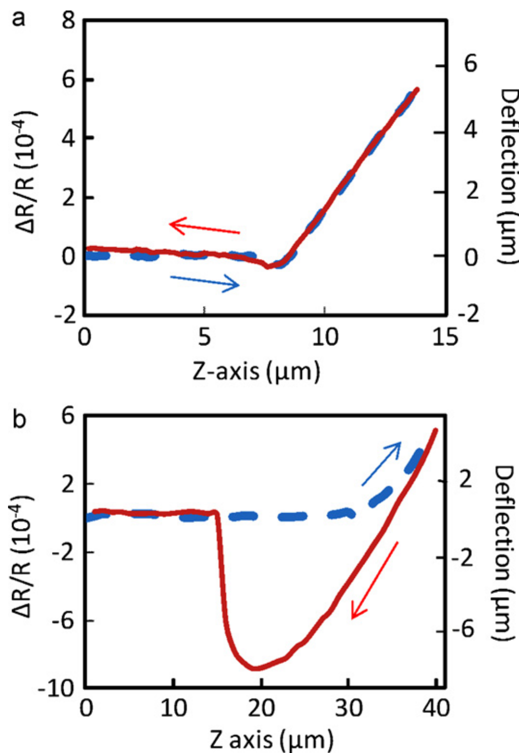

Fig. 3. Measured $\Delta R/R$ vs. out-of-plane probe movement (similar to an AFM force-curve) on two different materials. Force-curves on: (a) a glass substrate; (b) an elastomer (C6-235). The arrows indicate the direction of the movement. The blue thick dashed line represents the trace (probe and sample moving toward each other) and the red thin line represents the re-trace (probe and sample moving away from each other). The vertical axes are $\Delta R/R$ on the left and corresponding calculated cantilever deflection on the right, and the horizontal axis is the *Z*-axis movement of the sensing element toward and away from the sample. (For interpretation of the references to color in this figure legend, the reader is referred to the web version of the article.)

sion and elasticity). Typically, with an AFM, the cantilever is moved in *Z* axis toward the sample (trace) and then away from the sample (re-trace). The deflection of the cantilever is detected by a photodiode, plotted against the *Z*-axis scanner movement, and then analyzed.

The same capability can be realized by the micromachined piezoresistive probe, without the need of the complicated optical pickup used in the AFM. Resistance vs. displacement curves are produced using the probe and samples on the *XYZ* piezoelectric stage. The change in resistance can then be translated into the change in force as described in [13], which can be further used to extract the attractive and repulsive forces, as well as corresponding material properties. Besides the benefit of simplified signal readout, the closed-loop piezoelectric *XYZ* stage also provides larger measurement and interaction range (>40 μm), while in an AFM this range is typically limited by the piezoelectric tube scanner to ≈5 μm.

Curves of the change in the probe resistance with displacement in *Z*-axis on two different materials are shown in Fig. 3. Fig. 3a is a curve on a glass substrate and Fig. 3b is on an elastomer (Dow Corning, C6-235). At a *Z*-axis value of 0 μm the probe tip is not touching the sample. As the value on the *Z*-axis increases, the sample is brought closer to the tip. An attractive force deflects the probe toward the sample and thus there will be a decrease in the resistance of the element. A repulsive force deflects the probe away from the sample and there will be an increase in resistance. As can be seen in Fig. 3a and b, when the probe gets very close to the sample, it jumps into contact when it feels a sufficiently strong attractive force from the sample. As soon as the tip is in contact with the sample, the probe starts being pushed into the sample and the deflection will increase. This is translated into an increase in the slope of the curves in Fig. 3, which indicates that contact occurs around a value of 8.2 μm on the Z-axis for Fig. 3a and 31 μm for Fig. 3b. These values are arbitrary because the initial probe–sample distance is randomly chosen for this experiment. The slope and shape of the line is a measure of the elasticity of both the sample and the probe. The slope of the line on hard glass is 0.0553 Ω/μm (Fig. 3a), while the slope on the elastomer is 0.0304 Ω/μm (Fig. 3b), demonstrating, as expected, that the elastomer is more elastic than glass. The deflection sensitivity of the probe ($(\Delta R/R)/\Delta z$) can be extracted from the slope of the curve on glass and is ≈0.1 ppm/nm. Using Eq. (2) and the experimental data shown in Fig. 3a, the gauge factor of the metal piezoresistive sensor is calculated at 4.1 ± 0.1.

After reaching a certain predetermined *Z*-axis value the sample is moved away from the probe (re-trace). Initially, the curve is similar to the trace curve (approach), because the adhesive forces cause the probe to stay adhered to the sample even after passing the initial contact point. It can be seen that adhesive forces between the probe and the glass sample (Fig. 3a) are weaker than the forces on the elastomer (Fig. 3b). After moving a further distance away from the sample the adhesion is broken, and this value corresponds to the rupture force to break the adhesion from the surface. For Fig. 3a this value represents a change in resistance of $\Delta R = 0.0106\,\Omega$ or a $\Delta z \approx 190$ nm and for Fig. 3b represents a change in resistance of $\Delta R = 0.4654\,\Omega$ or a $\Delta z \approx 8.37$ μm. As expected, the greater the adhesion the greater the value of ΔR as evidenced from the comparison between the two graphs.

Knowing the probe elasticity enables us to extract the sample elasticity from the measurement curve. Young's modulus of the elastomer can be derived from: the measured piezoelectric stage *Z*-axis movement, the cantilever's deflection (by converting the change in resistance to the change in distance based on the calibration data), the probe radius, and the cantilever's spring constant. From the equation provided by Soofi et al. [26] we can solve for Young's modulus, E:

$$E = \frac{0.75k(d-d_o)(1-\nu^2)}{\sqrt{r}[(z-z_o)(d-d_o)]^{3/2}} \tag{4}$$

where z is the measured piezoelectric stage *Z*-axis movement, z_o is the value of z at the probe contact point, d is the cantilever's deflection, d_o is the value of d at the probe contact point, k is the cantilever spring constant, ν is Poisson's ratio (assumed to be 0.5 for a soft and incompressible material such as the elastomer sample [26]), and r is the probe radius (100 nm). The cantilever spring constant is derived from the equation:

$$k = \frac{E_{Si}wt^3}{4L^3} \tag{5}$$

where E_{Si} is Young's modulus of silicon (185 GPa), w is the width of the cantilever (200 μm), t is the thickness of the cantilever (2 μm), L is the length of the cantilever (300 μm). The effect of the metal and oxide layers is ignored considering their much smaller thicknesses compared with that of the silicon layer. The spring constant is calculated to be ≈2.74 N/m. From Eqs. (4) and (5) and from the measured data presented in Fig. 3b, Young's modulus of the elastomer is 2.6 ± 1.0 MPa, which is close to the manufacturer's published value of ≈1.4 MPa [27]. The discrepancy may be caused by the uncertainty in the spring constant, tip diameter, and Poison's ratio. Calibration can be performed to further improve the accuracy of the measurement.

5. Conclusion

In conclusion, a cantilever probe with an ultrathin film metal sensor is developed for scanning probe microscopy and material characterization. The probe has a very large dynamic range,

enabling monitoring movement of tens of microns in the out-of-plane axis. The rectangular cantilever is 200 μm wide and 300 μm long. It is made from silicon and silicon oxide with a total thickness of 2 μm and a 5 nm gold deflection sensing element. The gauge factor of the probe is 4.1 ± 0.1. Topographical scan capabilities were demonstrated. Plots of the change in resistance and cantilever deflection with the displacement of the sensing element on different materials demonstrate that the probe can be used to distinguish between materials with different mechanical properties. Furthermore, the probe was used to estimate Young's modulus of the elastomer studied.

Acknowledgments

We are grateful to Prof. Yogesh Gianchandani, Prof. Paddy French, and Dr. Cheryl Albus for their useful advice and help. This work was supported by the National Science Foundation (Award No. 0822810).

References

[1] T.R. Albrecht, S. Akamine, T.E. Carver, C.F. Quate, Microfabrication of cantilever styli for the atomic force microscope, J. Vac. Sci. Technol. A: Vac. Surf. Films 8 (4) (1990) 3386–3396, doi:10.1116/1.576520.
[2] A. Majumdar, P.I. Oden, J.P. Carrejo, L.A. Nagahara, J.J. Graham, J. Alexander, Nanometer-scale lithography using the atomic force microscope, Appl. Phys. Lett. 61 (1992) 2293, doi:10.1063/1.108268.
[3] H.J. Mamin, D. Rugar, Thermomechanical writing with an atomic force microscope tip, Appl. Phys. Lett. 61 (1992) 1003, doi:10.1063/1.108460.
[4] H.J. Mamin, B.D. Terris, L.S. Fan, S. Hoen, R.C. Barrett, D. Rugar, High-density data storage using proximal probe techniques, IBM J. Res. Dev. 39 (1995) 681–699, doi:10.1147/rd.396.0681.
[5] E.-L. Florin, M. Rief, H. Lehmann, M. Ludwig, C. Dornmair, V.T. Moy, H.E. Gaub, Sensing specific molecular interactions with the atomic force microscope, Biosens. Bioelectron. 10 (9–10) (1995) 895–901.
[6] K.D. Costa, Single-cell elastography: probing for disease with the atomic force microscope, Dis. Markers 19 (2004) 139–154.
[7] B. Bhushan, Handbook of Micro/Nanotribology, CRC Press, Boca Raton, 1999.
[8] R.B. Fair, V.K. Pamula, Detection of nanogram explosive particles with a MEMS sensor, Proc. SPIE 3710 (1999) 321.
[9] B.W. Chui, H.J. Mamin, B.D. Terris, T.D. Stowe, D. Rugar, T.W. Kenny, Low-stiffness silicon cantilevers for thermal writing and piezoresistive readback with the atomic force microscope, Appl. Phys. Lett. 69 (1996) 2767, doi:10.1063/1.117669.
[10] B.W. Chui, T.D. Stowe, Y.S. Ju, K.E. Goodson, T.W. Kenny, H.J. Mamin, B.D. Terris, Low-stiffness silicon cantilevers with integrated heaters and piezoresistive sensors for high-density AFM thermomechanical data storage, J. Microelectromech. Syst. 7 (1) (1998) 69–78, doi:10.1109/84.661386.
[11] M. Tortonese, R.C. Barrett, C.F. Quate, Atomic resolution with an atomic force microscope using piezoresistive detection, Appl. Phys. Lett. 62 (1993) 834, doi:10.1063/1.108593.
[12] M. Li, H.X. Tang, M.L. Roukes, Ultrasensitive NEMS-based cantilevers for sensing, scanned probe, and very-high frequency applications, Nat. Nanotechnol. 2 (2007) 114–120, doi:10.1038/nnano.2006.208.
[13] M Calleja, P.A. Rasmussen, A. Johansson, A. Boisen, Polymeric mechanical sensors with piezoresistive readout integrated in a microfluidic system, Proc. SPIE 5116 (2003) 314, doi:10.1117/12.498934.
[14] J.L. Arlett, M.L. Roukes, Ultimate and practical limits of fluid-based mass detection with suspended microchannel resonators, J. Appl. Phys. 108 (2010) 084701.
[15] A. Wisitsoraat, V. Patthanasetakul, T. Lomas, A. Tuantranont, Low cost thin film based piezoresistive MEMS tactile sensor, Sens. Actuators A 139 (2007) 17–22.
[16] O.J. Gregory, T. You, Stability and piezoresistive properties of indium-tin-oxide ceramic strain gages, Sensors 2 (2003) 801–806, ISBN:0-7803-8133-5.
[17] N.J. Allen, D. Wood, M.C. Rosamondb, D.B. Sims-Williams, Fabrication of an in-plane SU-8 cantilever with integrated strain gauge for wall shear stress measurements in fluid flows, Procedia Chem. 1 (September (1)) (2009) 923–926.
[18] E. Peiner, A. Tibrewala, R. Bandorf, S. Biehl, H. Lüthje, L. Doering, Micro force sensor with piezoresistive amorphous carbon strain gauge, Sens. Actuators A: Phys. 130–131 (2006) 75–82.
[19] A. Gaitas, W. Zhu, N. Gulari, E. Covington, C. Kurdak, Characterization of room temperature metal microbolometers near the metal-insulator transition regime for scanning thermal microscopy, Appl. Phys. Lett. 95 (2009) 153108, doi:10.1063/1.3250434.
[20] A. Johansson, M. Calleja, P.A. Rasmussen, A. Boisen, SU-8 cantilever sensor system with integrated readout, Sens. Actuators A: Phys. 123–124 (2005) 111–115.
[21] C. Li, P. Hesketh, G. Maclay, Thin gold film strain gauges, J. Vac. Sci. Technol. A12 (3) (1994) 813.
[22] M.-H. Li, Y.B. Gianchandani, Microcalorimetry applications of a surface micromachined bolometer-type thermal probe, J. Vac. Sci. Technol. B 18 (3600) (2000), doi:10.1116/1.1313581.
[23] J. Thaysen, Ph.D. thesis, Technical University of Denmark, 2001.
[24] D. Sarid, Scanning Force Microscopy: With Applications to Electric, Magnetic, and Atomic Forces I–XI, Oxford University Press, New York, 1991, p. 253.
[25] S. Akamine, R.C. Barrett, C.F. Quate, improved atomic force microscope images using microcantilevers with sharp tips, Appl. Phys. Lett. 57 (1990) 316, doi:10.1063/1.103677.
[26] S.S. Soofi, et al., J. Struct. Biol. 167 (September (3)) (2009) 216–219.
[27] www.dowcorning.com/DataFiles/090007c8801c2d86.pdf.

Biographies

Angelo Gaitas is the CEO of PicoCal Inc. He is pursuing a Ph.D. in industry with Delft University of Technology and is the principal investigator of this NSF funded research project. He received an M.B.A. from the University of Wisconsin at Madison, and an M.S. in Solid-State Physics from the University of London. His research interests lie in microcantilevers for scanning probe microscopy, manufacturing, chemical and biological applications.

Tao Li received a B.S and M.S in Engineering – Precision Instruments from Tsinghua University in Beijing, China in 2000 and 2002, respectively, and a Ph.D. in Electrical Engineering from the University of Michigan, Ann Arbor, in 2009. He works as a Postdoctoral Research Fellow at the University of Michigan, Ann Arbor and as a Research Scientist at PicoCal Inc.

Weibin Zhu received a B.S. degree in mechatronic engineering from the South China University of Technology, Guangzhou, China, in 1999, M.S. and Ph.D. degrees in mechanical engineering from the University of Michigan, Ann Arbor, in 2004 and 2009, respectively. As a Ph.D. student he developed a micromachined Joule-Thomson cryocooler for cryosurgical instruments. He is currently a Research Scientist at PicoCal Inc., where he is involved in MEMS projects related to scanning probe microscopy, biological and chemical sensing using microcantilevers.

Please cite this article in press as: A. Gaitas, et al., A probe with ultrathin film deflection sensor for scanning probe microscopy and material characterization, Sens. Actuators A: Phys. (2011), doi:10.1016/j.sna.2011.04.023